FUDMA Journal of Engineering and Technology
ISSN: 3092-9385
https://fjet.fudutsinma.edu.ng/index.php/fjet/
Volume 2, Issue 1, 2026, 442-452

Design Analysis of a Kenaf Decorticating Machine

Ibrahim BALA[1*], Solomon M. DAUDA[2], Audu A. BALAMI[3], Peter A. IDAH[4]

[1*,2,3,4]Department of Agricultural and Bioresource Engineering, Federal University of Technology, Minna, Nigeria

[1*]balaibrahimkt58@gmail.com, [2]smdauda@futminna.edu.ng, [3]aabalami@futminna.edu.ng, [4]pabaidah@yahoo.co.uk

Abstract

Kenaf (Hibiscus cannabinus L.) is a plant rich with fibre characterised with high growth rate that has the potential to replace synthetic and wood-based fibres. Traditional stalk fibre extraction (which is often manual) are tedious, ineffective and produce fibre qualities that are inconsistent in overall quality. This study describes the design analysis of a kenaf decorticating machine. Major components of the machine were identified and design data generated. Some of the design parameters were established, including the torque, stresses acting on the shafts, the belt tensions, decorticating and crushing forces and the required power needs, so as to increase processing efficiency and fibre yield. With a drum speed of 450 rpm, the machine decorticating force was obtained as 2,780 N, which is significantly greater than the determined crushing force of 695 N. Decortication was anticipated to require 7.9 kW of electricity, however the machine only required 282 W to run, indicating effective mechanical transmission. The pulley system and shaft diameter (35 mm) were selected to reduce energy loss and guarantee long-term operation. The machine has been designed to curtail the limitations of low decortication efficiency, excessive manual input, and safety concerns recorded from existing machines. The machine provides a practical solution for small- to medium-scale kenaf farmers, with the potential to revitalize local fibre industries and reduce environmental reliance on synthetic materials.

Keywords: *Decortication force, design analysis, fibre extraction, fibre-rich plant, mechanical transmission.*

1.0 Introduction

Kenaf (*Hibiscus cannabinus L.*) is a rapid-growing, annual, herbaceous bast fibre crop from the Malvaceae family (Akinrotimi and Okocha, 2018). It is closely related to cotton (*Gossypium hirsutum L.*) and okra (*Abelmoschus esculentus L.*) (Akinrotimi and Okocha, 2018). Kenaf matures at about 100 to 150 days and is planted across tropical and temperate climates. It is known locally in Nigeria as *Kerenkere* by the Igbo, *Ewe okun* in Yoruba and *Rama* in Hausa cultures (Dauda *et al.*, 2014). The structure of the plant is containing the leaves, flowers, seeds, and stalks. The overall plant structure has economic value; however, the stalk, which accounts for approximately 74% of the total biomass, is the primary source of industrial fibre (Xu, J., Tao, A., Qi, J. & Wang, Y., 2020). The stalk is comprised of the bast and the core. The core makes up to 35% of the stalk and reaches a length of 2 to 3 mm; it is highly crystalline, and rich in cellulose. The core on the other hand is about 65% of the stalk; it contains shorter fibres and is more lignin-rich (Austin *et al.*, 2019).

The kenaf plant been cultivated for over 6,500 years and originates in northern Africa. It was used in ancient Egypt around 1000 BC for fibre and food as reported by (Islam, 2019). Kenaf is a relatively small crop in Nigeria even though it is popular in the northern and southern parts of the country. Cultivars like Ifeken D1 4000 and Ifeken 400 are often used in these regions (Amusat *et al.*, 2014; Aminu, 2020). The crop has been reportedly used to make paper, textiles, ropes, and jute bags (Ibrahim and Ogunwusi, 2017; K. Oloruntoba and Jolaoso, 2017). Even though, some reports show it is also prevalently used in the production of biocomposites, solid biofuels, potting soil, and medicine, including blood pressure and cholesterol control (Ezzadin *et al.*, 2022; Vayabari *et al.*, 2023).

China and India are the dominant producers of kenaf with total production capacity reaching 70% (Alexopoulou *et al.*, 2013; Austin *et al.*, 2024). The production capacity of Nigeria is limited to about only 1,000 tonnes annually, even though, the potential is available for large scale production. This meagre production output may be

Received: 31/03/2026; Revised: 19/04/2026; Accepted: 20/04/2026; Published: 25/04/2026

attributed to limited commercial utilization, lack of investment, and inefficient processing systems (Olanipekun and Togun, 2020; Olasoji *et al.*, 2014).

The prevalent method of kenaf fibre extraction in Nigeria is labour-intensive and time-consuming. It also results in production of uneven fibre. Chemical retting for instance, might weaken the integrity of the fibre, while biologically retted fibres have superior mechanical qualities as reported by (Yu and Yu, 2010; Hossain *et al.*, 2022). Mechanical decortication, therefore, presents a viable alternative for improving processing efficiency, fibre consistency and quality.

There has been attempts at fabricating kenaf decorticating machines locally, however, they are characterized by low efficiency, frequent clogging, and unsafe design, including exposed moving parts. They are often immobile, expensive, and impractical for smallholder use (Austin *et al.*, 2024; Oyegbami and Ajijola, 2019). Fibre extraction alone contributes to about 16.9 to 20% of total production costs, further discouraging commercial cultivation (Palanikumar *et al.*, 2023; Onuwe *et al.*, 2018).

This paper presents the design analysis of a power-operated kenaf decorticating machine developed to address these challenges. The machine is designed to be affordable, safe, efficient, and suitable for local fabrication. By improving the processing of kenaf, it helps reduce production costs, enhance fibre quality, and boost the economic prospects of kenaf cultivation in Nigeria.

2.0 Materials and Methods

2.1 Materials

The materials to be used in the construction include mild steel plates, mild steel pipes, mild steel C-section, hardened tool steel and gears for transmission.

2.2 Method

2.2.1 Design Considerations

The following factors were considered in the design of the kenaf decorticating machine:

1. The machine was designed to ensure continuous operation with minimal idle time in order to improve productivity and fibre output.
2. Standard mechanical components such as belts, pulleys, and gears were adopted to reduce cost, simplify fabrication, and enhance flexibility.
3. The design ensures smooth material flow through the decorticating unit to minimize blockage and fibre loss during operation.
4. Locally available materials were selected to reduce production and maintenance costs and enhance accessibility for local users.
5. The selected materials and components were designed to possess adequate strength to withstand forces generated during crushing and decortication.
6. The machine was designed to ensure minimal loss of fibre during processing.
7. Materials used in fabrication were selected to avoid contamination of the extracted kenaf fibre.
8. The design minimizes labour requirement and operator fatigue, ensuring ease of operation.
9. The ratio of machine weight to working load was optimized to ensure efficient power utilization and ease of handling.

2.3 Design Analysis

The objective of the design analysis was to generate the necessary design data required for fabrication of the machine, ensuring reliability, efficiency, durability, safety, and affordability for the end users.

2.3.1 Determination of decorticating force

The decorticating force is produced as kenaf is squeezed between the top and lower decorticating drums. Equation 1 is used to calculate the decorticating force for an 8 stem per load feed input,

$$F_d = N_s F_c \quad (1)$$

where F_d is the decorticating force in N, N_s is the maximum number of kenaf stalk and F_c is the crushing force of the kenaf stalk in N.

2.3.2 Determination of power required for decortication

The power required for decortication is obtained with Equation 2 as provided by (Balami *et al.*, 2015),

$$P_d = \frac{2\pi N_d T_r}{60} \quad (2)$$

where P_d is the power required for decortication in W, N_d is the speed of the decorticating drum in rpm and T_r is the torque in Nm. The torque T_r is determined using Equation 3 (Khurmi and Gupta, 2012),

$$T_r = F_d r_d \quad (3)$$

Received: 31/03/2026; Revised: 19/04/2026; Accepted: 20/04/2026; Published: 25/04/2026

where r_d is the radius in m.

2.3.3 The machine belt drive selection

The V-belt drive is selected in this design analysis. It simplifies machine design, reduces cost and is highly efficient in use. The system consists of the driver and driven pulleys and a belt (Khurmi and Gupta, 2012).

2.3.3.1 Selection of pulley diameters

(Abdulkadir *et al.*, 2009) recommends belt type B as the belt type can carry load range of 2 to 15 kW. This is adequate for the power obtained which is 7.9 kW. The recommended minimum driver pulley diameter for the same range of power is 125 mm (Abdulkadir *et al.*, 2009). Subsequently a 150 mm pulley was selected and Equation 4 was used to determine the driven pulley diameter,

$$N_1 D_1 = N_2 D_2 \quad (4)$$

where N_1 and N_2 are the driver and driven pulley speeds in rpm respectively, while D_1 and D_2 are the driver and driven pulley diameters in m respectively.

2.3.3.2 Determination of belt tension(s)

The maximum belt tension T_{max} in N was determined using the allowable safe stress as expressed in Equation 5 (Khurmi and Gupta, 2012).

$$T_{max} = \sigma . b . t \quad (5)$$

The allowable safe stress σ in MN/m^2, b and t are the thickness and width of the belt which in mm respectively.

2.3.3.3 Determination of belt speed

Belt speed was obtained as 9.4 m/s using the Equation 6 as given by (Khurmi and Gupta, 2012).

$$v_b = \frac{\pi D_1 N}{60} \quad (6)$$

Substituting the values into Equation 9.

Rubber belt reinforced with fibres is selected for the design analysis of the machine as it has high load carrying capacity, good heat resistance and excellent adhesion (Khurmi and Gupta, 2012). The centrifugal tension was determined with Equation 7 according to (Khurmi and Gupta, 2012),

$$T_c = m_b v^2 \quad (7)$$

where T_c is the centrifugal tension in N, m_b is the mass of the belt in kg, is given by the product of the area, length (per unit metre) and the density of the belt material.

Tension on the tight side T_1 as stated by (Khurmi and Gupta, 2012) is the difference between the maximum tension and the centrifugal tension as expressed in Equation 8,

$$T_1 = T - T_c \quad (8)$$

where T_1 is the tension on tight side in N.

Tension on the slack side, T_2 in N was determined using Equation 9 as given by Khurmi and Gupta (2012).

$$\frac{T_1}{T_2} = e^{\mu \theta_1 \operatorname{cosec} \beta} \quad (9)$$

(Khurmi and Gupta, 2012) also provided 0.3 as the coefficient of friction μ between belt and pulley for rubber belts with cast iron or steel pulleys. The included angle (2β) value for standard B type V- belt from Figure 1 is 38^o (Khurmi and Gupta, 2012).

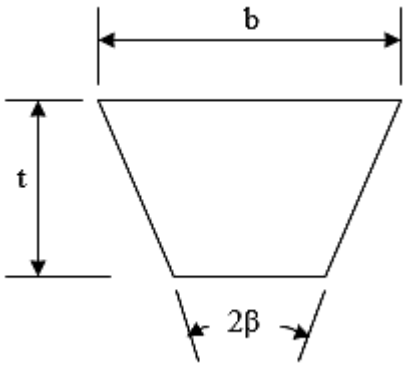

Figure 1: Cross section of a V-belt (Source: (Khurmi and Gupta, 2012))

θ_1 and θ_2 which are the contact angles were obtained using Equations 10 and 11 according to (Khurmi and Gupta, 2012).

$$\theta_1 = 180° - 2\alpha \quad (10)$$

$$\theta_2 = 180° + 2\alpha \quad (11)$$

But α is given by Khurmi and Gupta (2012);

$$\alpha = \sin^{-1}\left(\frac{R-r}{C}\right) \quad (12)$$

2.3.3.4 Determining the length of belt

Belt length is determined according to Khurmi and Gupta (2012) using Equation 13,

$$L_B = \frac{\pi}{2}(D_1 + D_2) + 2C_p + \left(\frac{D_1 - D_2}{4C}\right)^2 \quad (13)$$

where L_B is the belt length in m, D_1 is the driver pulley diameter in m, D_2 is the driven pulley diameter in m and C_p is the centre distance between pulleys in m.

2.3.3.5 Determination of the speed of the lower drum

As suggested by Fagbemi (2017), a speed ratio of 3:2 between the driven pulley and lower decorticating drums is adopted, it is expressed as Equation 14,

$$\frac{N_D}{N_l} = \frac{3}{2} \quad (14)$$

where N_D is the rotational speed of the driven pulley (450 rpm) and N_l is the rotational speed of the lower drum.

2.3.4 Analysis of gear drive

The minimum number of teeth on the pinion in order to avoid interference was determined using Equation 15 (Budynas *et al.*, 2015),

$$T_p = \frac{2A_w}{G\left[\sqrt{1+\frac{1}{G}\left(\frac{1}{G}+2\right)\sin^2\emptyset} - 1\right]} \quad (15)$$

where T_p is the number of teeth on the pinion, A_w is the module and 1 is adopted and G is the gear ratio. The number of teeth on the gear T_G is obtained using Equation 16 (Budynas *et al.*, 2015).

$$T_G = GT_p \quad (16)$$

2.3.4.1 Determination of gear and pinion pitch circle diameters

The pitch circle diameters (PCD) for the gear and pinion are determined using the Equation 17 (Fagbemi, 2017),

$$C_G = \frac{D_G}{2} + \frac{D_p}{2} \quad (17)$$

where C_G is the centre distance in m, and 0.15 adopted (AutoCAD 2016 inquiry tool), D_G is pitch circle diameter of the gear in m and D_P is the pitch circle diameter of the pinion in m from the gear ratio of 1.5 Equation 18 is derived.

$$D_G = 1.5D_P \quad (18)$$

2.3.5 Determination of shaft diameter

Equation 19 was used to determine the shaft diameter (Egbe and Olugboji, 2016).

$$d^3 = \frac{16}{\pi S_s}\sqrt{(Mk_b)^2 + (Tk_t)^2} \quad (19)$$

where S_s is the shear stress, and it is taken as 42 MN/m² (Khurmi and Gupta, 2012), K_b and K_t are combined shock and fatigue bending and torsion factors respectively. According to Egbe and Olugboji (2016) combined shock and fatigue bending (K_b) and torsion (K_t) factors for suddenly applied load, minor shock are 1.5-2 and 1-1.5 respectively.

The decorticating drum was designed as a hollow cylindrical component fabricated from mild steel. The mass of the drum was determined based on its geometric dimensions and material density. The volume of a hollow cylinder is given by Equation 20,

$$V = \frac{\pi L}{4}(D_o^2 - D_i^2) \quad (20)$$

where V is the volume of the drum (m³), L is the length of the drum (m), $D_o$is the outer diameter (m) and D_i is the inner diameter (m).

The mass of the drum was then determined using Equation 21.

$$m = \rho V \quad (21)$$

where m is the mass of the drum (kg) and ρ is the density of mild steel (kg/m³)

Received: 31/03/2026; Revised: 19/04/2026; Accepted: 20/04/2026; Published: 25/04/2026

3.0 Results and Discussion

3.1 Design analysis results

3.1.1 Decorticating force

The crushing force of 4 kenaf stalk is 694.86 N for 72% moisture content according to Equation 1 (Dauda *et al.*, 2014).

$$F_d = 4 \times 694.86$$

$$F_d = 2{,}779.5 \text{ N}$$

3.1.2 Power required for decortication

The power required for decortication is obtained with Equation 3. Fagbemi (2017) and Karim *et al.* (2021) suggested a speed of 450 rpm adequate for decorticating drum rotation that will give efficcient decortication. The torque T_r is determined using Equation 3 with the radius of the decorticating drum being 0.060 m. the power was hence, determined as 7.9 kW.

$$T_r = 2{,}779.5 \times 0.060$$

$$T_r = 166.8 \text{ Nm}$$

The power is thus obtained as

$$P_d = \frac{2 \times \pi \times 450 \times 166.8}{60}$$

$$P_d = 7{,}860 \text{ W or } 7.9 \text{ kW}$$

3.1.3 Selection of pulley diameters

N_1 is the engine speed which is 1,200 rpm, N_2 is 450 rpm as suggested by Karim *et al.* (2021) and D_1 is 0.15 m, so, D_2 is determined to be 0.4 m using Equation 4.

$$D_2 = \frac{1{,}200 \times 0.15}{450}$$

$$D_2 = 0.4 \text{ m}$$

3.1.4 Belt tension(s)

The allowable safe stress σ is adopted as 2.1 MN/m^2 (Khurmi and Gupta, 2012), b and t are the thickness and width of the belt which are 17 mm and 11 mm respectively (Abdulkadir *et al.*, 2009).

$$T_{max} = 2.1 \times 10^6 \times 0.017 \times 0.011 = 392.7 \text{ N}$$

3.1.5 Belt speed

Using Equation 6 along with electric motor speed of 1200 rpm, the belt speed is obtained as 9.4 m/s.

$$v_b = \frac{\pi \times 0.15 \times 1200}{60}$$

v_b = 9.4 m/s

The centrifugal tension was determined with Equation 7 according to Khurmi and Gupta (2012). Rubber density according to Khurmi and Gupta (2012) is 1140 kg/m^3.

$$T_c = 0.017 \times 0.011 \times 1 \times 1140 \times 9.4^2 = 18.84 \text{ N}$$

Tension on the tight side T_1 as stated by Khurmi and Gupta (2012) is the difference between the maximum tension and the centrifugal tension as expressed in Equation 8.

$$T_1 = 392.7 - 18.84$$

$$T_1 = 373.86 \text{ N}$$

Tension on the slack side, T_2 in N was determined using Equation 9 as given by Khurmi and Gupta (2012).

Khurmi and Gupta (2012) also provided 0.3 as the coefficient of friction μ between belt and pulley for rubber belts with cast iron or steel pulleys. Pulley diameters 400 mm and 150 mm and the distance between the pulleys is 500 mm from preliminary design drawing.

$$\alpha = \sin^{-1}\left(\frac{0.2 - 0.075}{0.50}\right)$$

$\alpha = 14.5^o$

The contact angles are obtained substituting the value 8.6^o into Equations 10 and 11.

$\theta_1 = 180° - 2 \times 14.5 = 151^o$ or 2.64 rad

$\theta_2 = 180° + 2 \times 14.5 = 209^o$ or 3.65 rad

$$\frac{T_1}{T_2} = e^{0.3 \times 2.64 \times \text{cosec}19}$$

Received: 31/03/2026; Revised: 19/04/2026; Accepted: 20/04/2026; Published: 25/04/2026

$T_2 = 32.91$ N

3.1.6 Length of belt

$$L_B = \frac{\pi}{2}(0.15 + 0.4) + 2 \times 0.5 + \left(\frac{0.15 - 0.4}{4 \times 0.5}\right)^2$$

$L_B = 1.88$ m = 1,880 mm

So, the belt type B with length 1,880 mm was selected. `

3.1.7 Speed of the lower drum

N_D is the rotational speed of the driven pulley (450 rpm).

$N_l = \frac{N_u \times 2}{3}$

$N_l = \frac{450 \times 2}{3}$

$N_l = 300$ rpm

3.1.8 Analysis of gear drive

The gear ratio, 1.5 is adopted (Fagbemi, 2017). $\emptyset$ is the pressure angle and 20° is adopted for the gear.

$$T_p = \frac{2 \times 1}{1.5\left[\sqrt{1 + \frac{1}{1.5}\left(\frac{1}{1.5} + 2\right)\sin^2(20) - 1}\right]}$$

$T_p = 13.33$

The number of teeth on the gear T_G is obtained using Equation 16 as 21.

3.1.9 Gear and pinion pitch circle diameters

$0.15 = \frac{1.5 D_P}{2} + \frac{D_p}{2}$

$D_P = 0.12$ m

$D_G = 1.5 \times 0.12$

$D_G = 0.18$ m

The gear pitch circle diameter and pinion pitch circle diameter are obtained as 0.18 and 0.12 m respectively.

3.1.10 Determination of shaft diameter

Equation 19 was used to determine the shaft diameter (Egbe and Olugboji, 2016). The free body diagram of the shaft is provided in Figure 2, it illustrates the vertical forces acting on the shaft, which are considered first. For the design of the decorticating drum the following parameters were used for the conceptualised machine design: outer diameter, $D_o = 0.04$ m, inner diameter, $D_i = 0.03640$ m and length, $L = 0.60$ m.

$V = \frac{3.142 \times 0.60}{4}(0.0400 - 0.03640)$

$V = 0.4712 \times 0.00360$

$V = 0.001695$ m^3

Density of mild steel is 7850 kg/m^3 as stated by Egbe and Olugboji (2016).

$m = 7850 \times 0.001695$

$m = 13.3$ kg

This value is equal to 13.3 kg or 130.5 N.

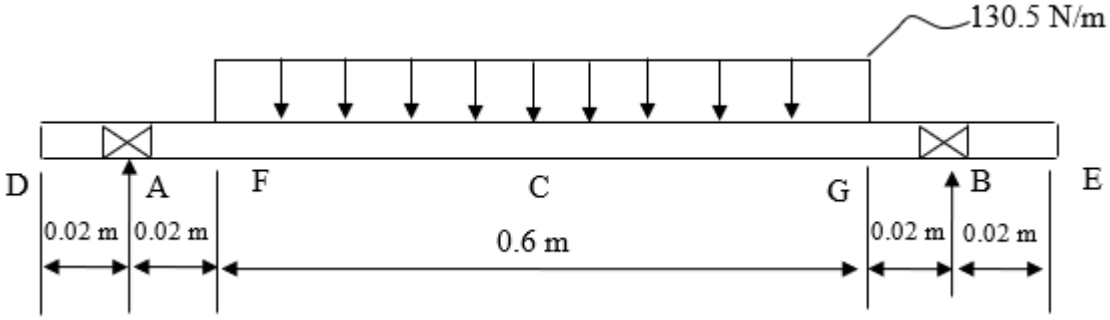

Figure 2: Vertical forces acting on the shaft

The resultants for the vertical forces R_{AV} and R_{BV} at points A and B was obtained by first determining the total load distribution.

$$W_N = w_N \times (0.64 - 0.04) \quad (22)$$

where W_N is the total distributed load in N and w_N is the distributed load in N/m.

$W_N = 130.5 \times (0.64 - 0.04) = 78.3$ N

The centroid at point C on Figure 2 is determined with Equation 23 as 0.34 m.

$$x_{centroid} = \frac{0.64+0.04}{2} \quad (23)$$

Applying equilibrium conditions, the sum of vertical forces $\sum = 0$.

$$R_{AV} + R_{BV} = 78.3 \text{ N} \quad (24)$$

Also, sum of moments about point A ($\sum M = 0$) is carried out.

$R_{BV} \times (0.66 - 0.02) = 78.3 \times (0.34 - 0.02)$

$R_{BV} = 39.15$ N

R_{AV} is obtained as 39.15 N from Equation 24.

The shear force ($V(x)$) at any point along the beam was determined by considering the reactions and the distributed load.

For $x = 0.02$ to 0.04

$V(x) = R_{AV} = 39.15$ N

For $x = 0.04 \leq x \leq 0.64$

$V(0.04) = 39.15$ N, $V(0.34) = 0, V(0.64) = -39.15$ N

For $x = 0.64$ to 0.66

$V(x) = 39.15 - 39.15 - 78.3 = -39.15$ N

The bending moment $M(x)$ at any point is calculated by integrating the shear force.

For $x = 0.02 \leq x \leq 0.04$

$M(0.02) = 0, M(0.04) = 0.783$ Nm,

For $x = 0.04 \leq x \leq 0.64$

$M(0.34) = 6.66$ Nm, $M(0.64) = 0.783$ Nm

For $x = 0.64 \leq x \leq 0.66$

$M(0.66) = 0$

Figure 3 depicts the horizontal forces acting on the shaft. The belt tension acts on this plane. T_1 and T_2 were calculated as 373.86 and 32.91 N respectively.

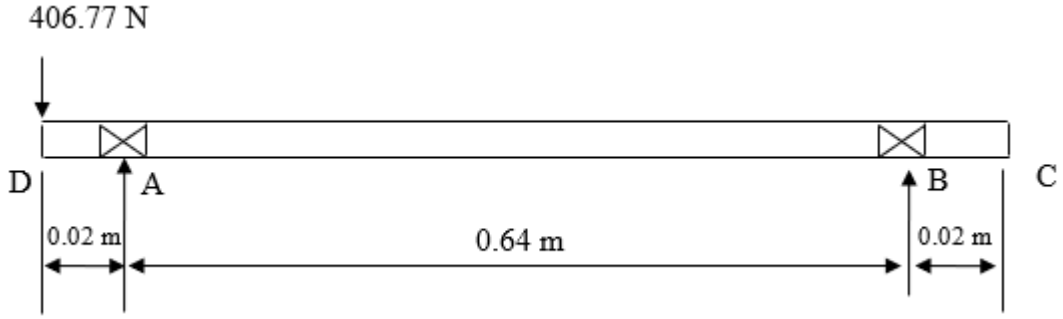

Figure 3: Horizontal forces acting on the shaft

The reaction at the supports is obtained by summing the vertical forces and taking moment about point A.

$$R_{AH} + R_{BH} = 406.77 \text{ N} \quad (25)$$

$R_{BH} \times (0.66 - 0.02) = 406.77 \times 0.02$

$R_{BH} = 12.71$ N

From Equation 25 R_{AH} is obtained as 394.06 N

For $x = 0, V(0.02) = -12.71$ N

For $x = 0.66$ m, $V(x) = -12.71 + 12.71 = 0$

The bending moment at any point along the shaft was found by integrating the shear force. The bending moment at the supports A and B (for simply supported beams) is 0.

For $x = 0, M(0) = 0, M(0.34) = -4.07$ Nm, $M(0.64) = -7.88$ Nm and $M(0.66) = -8.13$ Nm

The bending moment is 0 at the support.

The resultant bending moment was then obtained for each points A, F, C, G and B as 0 Nm, 8.17 Nm, 7.81 Nm, 7.92 Nm and 0 Nm respectively. Hence, the maximum bending moment is 8.17 Nm. The shear force and bending moments are represented in Figure 4. The torque T_r, is 166.8 Nm and substituted into Equation 19.

$$\mathrm{d}^3 = \frac{16}{\pi \times 42 \times 10^6}\sqrt{(8.17 \times 1.5)^2 + (166.8 \times 1)^2}$$

Received: 31/03/2026; Revised: 19/04/2026; Accepted: 20/04/2026; Published: 25/04/2026

$d = \sqrt[3]{2.03 \times 10^{-5}}$ = 0.027 m = 27 mm

The shaft diameter available for the machine is 35 mm, this is more than the calculated value obtained, and thus design is safe.

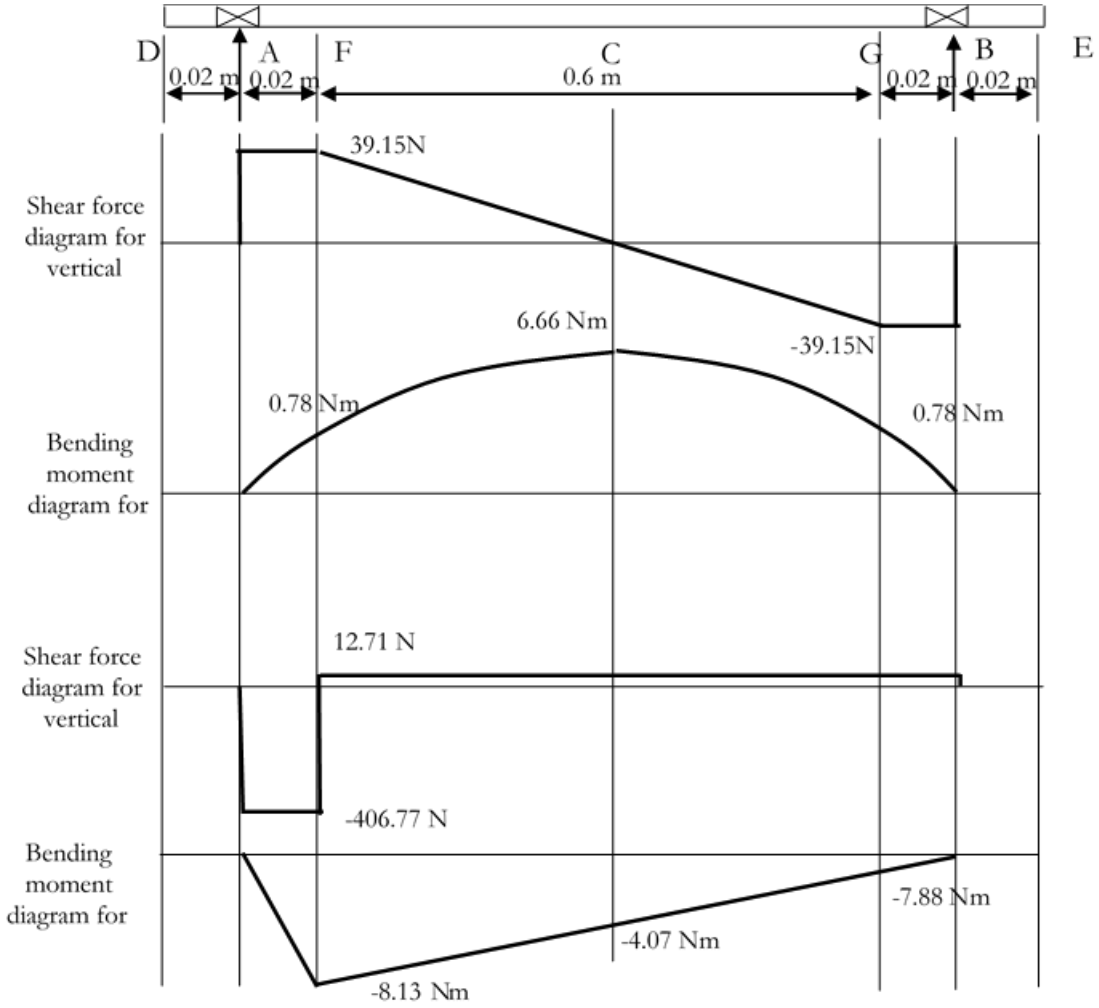

Figure 4: Shear force and bending moment diagram

The summary of the design analysis results generated from the study are presented in Table 1. The results describe the main parameters of the kenaf decorticating machine, offering a clear understanding of its operating efficiency and the strength of its overall design. The decorticating force of 2,779.5 N is much greater than the crushing force of 694.86 N, highlighting how demanding the decortication stage is compared to the initial crushing step.

Table 1: Summary of Design analysis results

S/N	Parameters	Value	Unit
1.	Crushing force	694.86	N
2.	Decorticating force	2,779.5	N
3.	Power required for decortication	7,860	W
4.	Drum speed	450	rpm
5.	Drum radius	0.06	m
6.	Torque	166.8	Nm
7.	Power required to drive the machine	281.92	W
8.	Maximum belt tension	392.7	N
9.	Driver pulley diameter	0.15	m

Received: 31/03/2026; Revised: 19/04/2026; Accepted: 20/04/2026; Published: 25/04/2026

S/N	Parameters	Value	Unit
10.	Driven pulley diameter	0.4	m
11.	Tension in tight side	373.86	N
12.	Tension in slack side	32.91	N
13.	Belt speed	9.4	m/s
14.	Centrifugal tension	18.84	N
15.	Belt length	1,880	mm
16.	Number of teeth on the pinion	14	-
17.	Number of gear teeth	21	-
18.	Maximum bending moment	8.17	Nm
19.	Shaft diameter	35	mm

Decortication requires 7,860 W of power, demonstrating the high energy demand of the process and the need for a reliable power source. In contrast, the machine itself operates on only 281.92 W, indicating that the mechanical transmission system is highly efficient and will effectively minimize energy losses during operation. The power requirement of 7.9 kW for decortication is also consistent with values reported in literature. A power-operated kenaf/jute fibre extraction system evaluated by Karim *et al.* (2021) reported approximately 9.48 kW engine power for effective operation. The close agreement between these values validates that the estimated power demand in this design is realistic and sufficient for fibre separation.

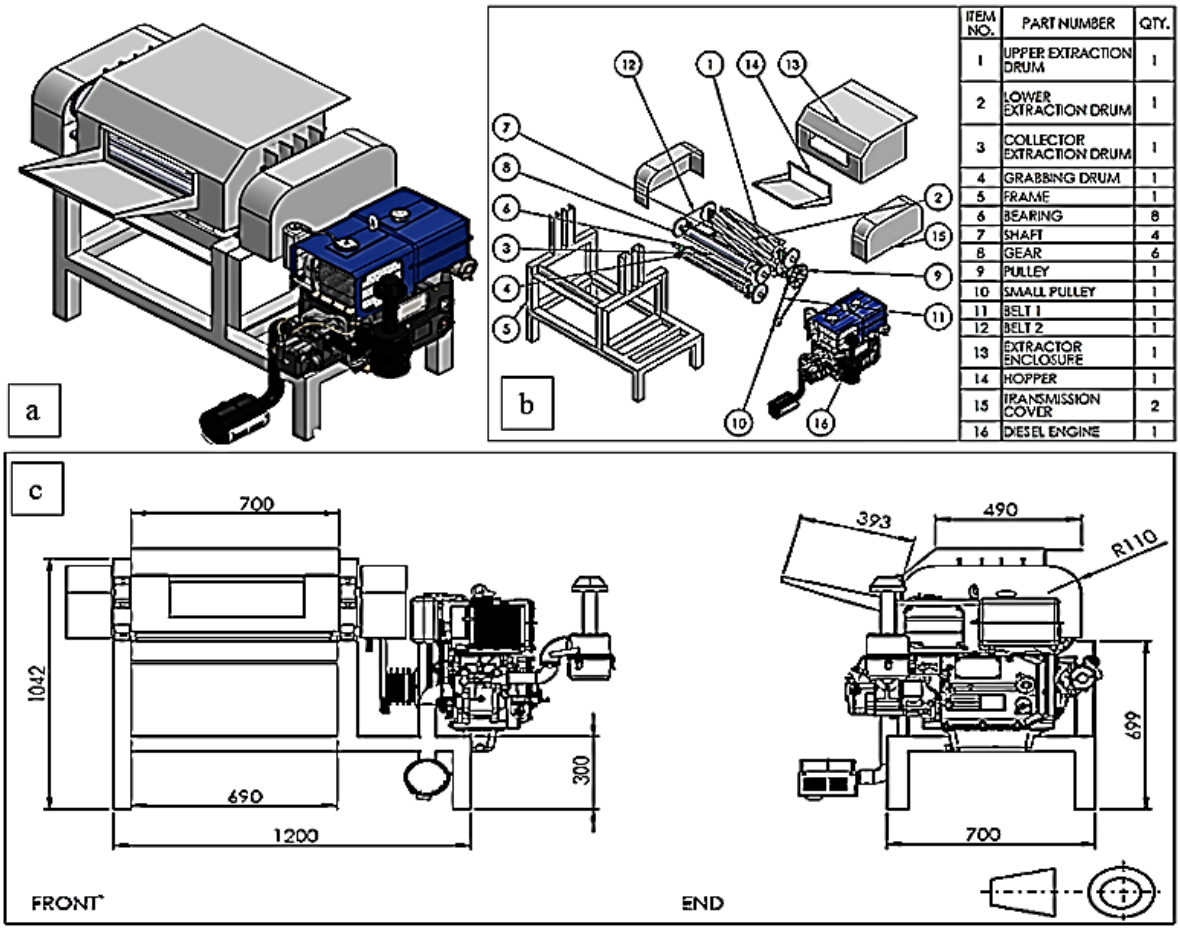

Figure 5: Design drawing of the designed machine

With a torque output of 166.8 Nm at 450 rpm and a radius of 0.06 m, the drum provides enough rotational force to keep the fibre-extraction process running smoothly without any stalling. The selected drum speed of 450 rpm aligns closely with values reported in experimental studies. For instance, a kenaf decorticator evaluated by Ayorinde and Owolarafe (2023) operated effectively within a speed range of 520–600 rpm, which was identified as optimal for fibre extraction. Similarly, Makanjuola *et al.* (2019) reported efficient operation at equivalent peripheral speeds corresponding to this rotational range. This shows that the adopted design speed falls within the practically validated operating window, confirming its suitability. The 35 mm diameter shaft is equally well-

Received: 31/03/2026; Revised: 19/04/2026; Accepted: 20/04/2026; Published: 25/04/2026

matched to the system, built to withstand a maximum bending moment of 8.17 Nm and deliver steady, durable performance throughout operation. The belt–pulley setup shows strong transmission efficiency, carrying a maximum belt tension of 392.7 N with a well-balanced distribution between the tight and slack sides. Its belt speed of 9.4 m/s and overall length of 1,880 mm indicate that the system is tuned for steady, trouble-free operation. The gear arrangement, featuring a 14:21 pinion-to-gear ratio, further supports this performance by delivering the required torque and rotational speed for effective machine operation.

The designed machine design drawing is presented in Figure 5 a. is the isometric drawing, b. is the exploded diagram, and c. is the orthographic projection of the machine.

4.0 Conclusion

The design analysis of the kenaf decorticating machine established the key mechanical parameters required for the development of a reliable and functional system for fibre extraction. The calculated decorticating force of approximately 2,780 N exceeds the crushing force of 695 N, confirming that the machine components are adequately sized to achieve effective fibre separation under expected operating conditions.

The power requirement for decortication was determined to be about 7.9 kW, while the machine drive system requires only 282 W, indicating that the selected transmission components are appropriately matched to ensure efficient power transfer. The belt and pulley arrangement, along with the gear system, were properly dimensioned to provide the required speed reduction and torque transmission necessary for continuous operation. The shaft diameter of 35 mm was found to be sufficient to withstand the combined bending and torsional loads, ensuring structural integrity and operational safety. Similarly, the selected materials and component dimensions satisfy strength and durability requirements for the anticipated loading conditions.

Overall, the design provides a technically sound basis for fabrication, with considerations for strength, safety, efficiency, and the use of locally available materials. The outcome of this analysis serves as a foundation for the construction and future testing of the machine.

References

Abdulkadir, B. H., Matthew, S. A., Olufemi, A. O., & Ikechukwu, C. U. (2009). The design and construction of maize threshing machine. *Assumption University Journal of Technology, 12*(3), 199-206.

Ailenokhuoria, B. V., Omena, E. C. & Isaac, O. O. (2020). Physicochemical composition of kenaf(Hibiscus Cannabinus L.) seed under different storage temparature. *Sustainability, Agri, Food and Environmental Research, 8*, 212-225.

Akinrotimi, C. A., & Okocha, P. I. (2018). Evaluations of genetic divergence in Kenaf (Hibiscus Cannabinus L.) genotypes using agro-morphological characteristics. *Journal of Plant Sciences and Agricultural Research, 2*(12), 2167–2412.

Alexopoulou, E., Christou, M., Papatheohari, Y. & Monti, A. (2013). Origin, description, importance, and cultivation area of kenaf. *Green Energy and Technology, 117*(1), 1-15.

Aminu, H. (2020). *Performance of kenaf (Hibiscus Cannabinus l.) varieties as influenced by poultry manure rate in the northern Guinea and Sudan Savannah.* Zaria: Ahmadu Bello University, Zaria.

Amusat, A. S. & Ademola, A. O. (2014). Information Needs of Kenaf Farmers in Ogbomoso Zone of Oyo State, Nigeria. *American Journal of Experimental Agriculture, 4*(12), 1625-1636.

Austin, C. C., Mondell, C. N., Clark, D. G. & Wilkie, A. C. (2024). Kenaf: Opportunities for an Ancient Fiber Crop. *Agronomy, 14*(7), 1-15.

Ayorinde, A., & Owolarafe, O. (2023). Effect of operational parameters on the performance of a kenaf harvester. *Spanish Journal of Agricultural Research*, 21(4), 1-10.

Balami, A. A., Dauda, S. M., Aliyu, M. & Muhammed, I. S. (2015). Development and performance evaluation of a neem seed decorticator. *Naigerian Journal of Engineering and Applied Sciences, 2*(1), 28-36.

Budynas, R. G., Nisbett, J. K. & Shigley, J. E. (2015). *Shigley's mechanical engineering design.* New York: McGraw-Hill.

Chakraborty, S. & Javed, S. A. (2017). Scenario of car wastes reusing and recycling in Dhaka city. *International Conference on Engineering Research, Innovation and Education* (pp. 140-145). Sylhet, Bangladesh: ICERIE .

Dauda, S. M., Ahmad, D., Khalina, A & Jamarei, O. (2014). Physical and mechanical properties of kenaf stems at varying moisture contents. *2nd International Conference on Agricultural and Food Engineering, CAFEi2014* (pp. 370-374). Selangor: CAFEi2014.

Dauda, S. M., Ahmad, D., Khalina, A., & Jamare, O. (2015). Effect of cutting speed on cutting torque and cutting power of varying kenaf-stem diameters at different moisture contents. *Tropical Agricultural Science, 38*(4), 549 - 561.

Egbe, E. A. P. & Olugboji, O. A. (2016). Design, fabrication and testing of a double roll crusher. *International Journal of Engineering Trends and Technology (IJETT), 35*(11), 2231-5381.

Ezzadin, N. A., Salih, R. F. & Sultan, D. M. . (2022). A comprehensive review on Kenaf seeds and leaves for medicine. *Journal of Medicinal Plants Studies, 10*(5), 26-33.

Received: 31/03/2026; Revised: 19/04/2026; Accepted: 20/04/2026; Published: 25/04/2026

Fagbemi, S. A. (2017). *Development and performance evaluation of a motorised kenaf (Hibiscus Cannabinus L.) stem decorticating machine.* Minna: FUT Minna.

Falana, O., Aluko, O., Adetan, D., & Osunbitan, J. (2019). The physical properties and strength characteristics of kenaf plants. *Research in Agricultural Engineering, 65*(4), 131–136.

Hossain, M. M., Subbiah, V. K. & Siddiquee, S. (2022). Augmented retting effect on kenaf fibers using alkalophilic pectinase-producing bacteria in combination with water solvents. *Applied Science, 12*(14), 1-12.

Ibrahim, H. D. & Ogunwusi, A. A. (2017). Prospects for Kenaf Textile Production in Nigeria. *Journal of Natural Sciences Research, 7*(1), 22-28.

Islam, M. M. (2019). Kenaf (hibiscus Cannabinus l., Malvaceae) Research and Development Advances in Bangladesh: a review. *Journal of Nutrition and Food Processing, 2*(1), 1-8.

Karim, R., Hoque, M. A., Chawdhury, A., Islam, F., Ahmed, S., Sabagh, A. & Hossain, A. (2021). Design, development, and performance evaluation of a power-operated jute fiber extraction machine. *AgriEngineering, 3*(2), 403-422.

Khurmi, R. S. & Gupta, J. K. (2012). *A textbook of machine design.* New Delhi, India: S. Chand & Company Ltd.

Makanjuola, G. A., Ayorinde, T. A., Aluko, O. B., Owolarafe, O. K. & Sanni, L. A. . (2019). Performance evaluation of a kenaf decorticator. *Agricultural Engineering International: CIGR Journal, 21*(1), 192-202.

Olanipekun, S. O. & Togun, A. O. (2020). Effect of Planting Date on the Growth, Fibre and Seed Yield of Kenaf (Hibiscus cannabinus L) in Ibadan, South Western Nigeria. *Journal of Applied Science and Environmental Management, 24*(10), 1711-1714.

Olasoji, J. O., Aluko, O. A., Agbaje, G. O., Adeniyan, O. N., Kareem, K. O. & Olanipekun, S. O. (2014). Studies on seed yield potential of some selected kenaf (Hibiscus cannabus L.) genotypes. *African Journal of Biotechnology, 13*(24), 2420-2424.

Oloruntoba, K. & Jolaoso, M. A. . (2017). *A monograph on production and processing of kenaf in Nigeria.* UK: LAP Lambert Academic.

Onuwe, J. O., Ogunbode, E. B., Jamaludin, M. Y. & Shettima, A. U. (2018). An overview of kenaf fibre as a bio composites material in fabrication process for sustainable construction. *Environmental Technology & Science Journal, 9*(1), 134-144.

Oyegbami, A. & Ajijola, S. (2019). Knowledge of the Potentials and Constraints in Kenaf Production among Farmers in Southwest Nigeria. *Moor Journal of Agricultural Research, 20*(2), 20(2), 189 - 197.

Palanikumar, K., Natarajan, E., Makandan, K., Ang, C. K. & Franz, G. (2023). Targeted pre-treatment of hemp fibers and the effect on mechanical properties of polymer composites. *Fibers, 11*(5), 1-12.

Uicker, J. J., Pennock, G. R. & Shigley, J. E. (2017). *Theory of machines and mechanisms* . New York: Oxford University Press.

Vayabari, D. A. G., Ilham, Z., Saad, N., Usuldin, S. R. A., Norhisham, D. A., Abd Rahim, M. H. & Wan-Mohtar, W. A. I. (2023). Cultivation Strategies of Kenaf (Hibiscus cannabinus L.) as a Future Approach in Malaysian Agriculture Industry. *Horticulturae, 9*(8), 1-18.

Xu, J., Tao, A., Qi, J. & Wang, Y. (2020). Bast fibres: kenaf. In .. M.-T. Kozłowski, *In Woodhead Publishing Series in Textiles, Handbook of Natural Fibres (Second Edition)* (pp. 71-92). UK: Woodhead Publishing.

Yu, H. & Yu, C. (2010). Influence of various retting methods on properties of kenaf fiber. *The Journal of the Textile Institute, 101*(5), 452-456.

Received: 31/03/2026; Revised: 19/04/2026; Accepted: 20/04/2026; Published: 25/04/2026